https://doi.org/10.46813/2025-157-094

CHARACTERISTICS OF LOW POWER RF ION SOURCE

V.I. Voznyi, A.G. Ponomarev, D.V. Magilin, D.P. Shulha, V.A. Rebrov
Institute of Applied Physics, National Academy of Sciences of Ukraine, Sumy, Ukraine
E-mail: vozny56@gmail.com

The main characteristics of a low-power inductive RF ion source designed for use in a compact nuclear microprobe at the IAP NASU are presented. The source operates at a frequency of 45 MHz with RF power below 10 W. The extracted beam current reaches up to 3.5 μA through a 0.6 mm diameter aperture. The beam is composed of $^1H^+$, $^2H^+$, and $^3H^+$ ions, and the proton ($^1H^+$) fraction is about 10%. The measured energy spread of the ion beam is in the range of 7.5…9 eV. The beam emittance is 9.8 π·mm·mrad, and the normalized emittance is 0.037 π·mm·mrad.

PACS: 29.25.Ni; 41.75.Ak; 41.85.Qg

INTRODUCTION

Modern nuclear microprobes represent advanced analytical end-stations, typically based on electrostatic accelerators, and are widely employed for non-destructive, high-resolution microanalysis as well as for the fabrication of three-dimensional micro- and nanostructures. In conventional setups, ion beams-usually hydrogen or helium-with currents up to 100 μA are accelerated to energies of several MeV [1–3]. These beams are then focused and collimated within a dedicated microprobe end-station. However, only a minor fraction of the beam, often limited to a few nanoamperes, is effectively utilized, resulting in inefficient use of the initial beam.

Furthermore, mass analysis of the beam is typically performed after acceleration, requiring large and power-intensive analyzing magnets. This design not only increases the system's energy consumption but also adds significantly to its cost. Importantly, the acceleration stage itself does not directly contribute to the microbeam formation; rather, the process begins effectively at the object collimator. To achieve high demagnification and spatial resolution, ion-optical systems often extend up to 10 m in length, with most of this distance consisting of drift spaces devoid of electromagnetic control fields.

To overcome these limitations, a concept for a compact nuclear microprobe was proposed at the Institute of Applied Physics of the NAS of Ukraine [4, 5]. This approach employs specialized ion sources with low beam currents (typically a few nA) and an energy spread of approximately 10 eV, aimed at reducing the effects of chromatic aberration. In low-energy ion beam systems, high-resolution performance is generally achieved using liquid metal ion sources or field emission sources. These sources generate a small ion emission region, often nanometer sizes. As a result, such ion sources exhibit much higher brightness compared to those used in general-purpose electrostatic accelerators [6]. However, due to their specific technical characteristics, these sources are not suitable for use in a compact microprobe.

Recently, an electron impact ion source with dimensions ranging from 0.1 to 1 μm was developed for the ion microprobe at the National University of Singapore [7, 8]. However, this source produces a beam of molecular ions ($^2H^+$) rather than protons ($^1H^+$), which are essential for standard techniques such as PIXE, RBS, and proton beam writing.

Radio-frequency (RF) plasma ion sources present a promising alternative for proton generation and are widely utilized in ion beam technologies [9–11]. When operating with hydrogen, RF ion sources can deliver beam currents up to 100 μA at 150 W RF power, with a proton fraction reaching 70%. However, a significant drawback is their high energy spread, which can reach around 100 eV [11].

In view of the above, a low-power inductive RF ion source has been designed at the IAP NAS of Ukraine for application in compact nuclear microprobe [12]. The source operates at RF power below 10 W and is intended for generating a $^1H^+$ ion beam required for standard techniques such as PIXE, RBS, and proton beam writing. The source will operate as part of the nuclear microprobe injector, along with a small-sized Wien filter and an einzel lens. The Wien filter is used to separate the proton component of the beam, while the einzel lens focuses the selected proton beam into a crossover, which can be used as an object for microprobe formation.

This article presents the experimental characterization of the developed ion source, including measurements of total ion current, mass composition, proton fraction, axial energy spread, and beam emittance.

1. RF ION SOURCE

The schematic of the inductive RF ion source is shown in Fig. 1. The source consists of a cylindrical quartz discharge tube with an outer diameter of 34 and a length of 70 mm. Surrounding the quartz tube is a copper induction coil consisting of six turns of 4 mm diameter wire. An RF voltage at a frequency of 45 MHz is applied to the coil to sustain plasma discharge.

Hydrogen gas is introduced into the quartz chamber at a pressure of approximately 1 Pa. The time-varying magnetic field generated by the coil induces an azimuthal RF electric field within the discharge volume. Free electrons within the gas absorb energy from the RF field, leading to collisional excitation and ionization of hydrogen molecules and the subsequent formation of plasma.

Positive ions generated in the discharge are extracted from the plasma through a dedicated extraction aperture. The extraction channel has a diameter of 0.6 and a length of 3 mm. A downstream acceleration electrode is employed to focus the extracted ion beam and provide the desired beam energy.

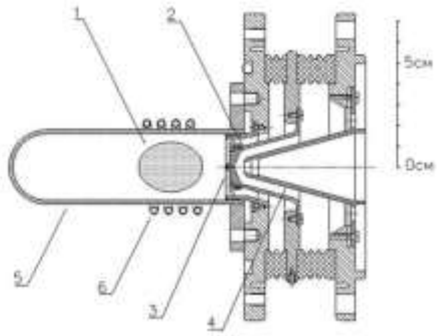

Fig. 1. Schematic diagram of the inductive RF ion source: 1 – plasma volume; 2 – extraction electrode; 3 – quartz diaphragm; 4 – acceleration (focusing) electrode; 5 – quartz discharge tube; 6 – induction coil

The ion current extracted from an inductively coupled plasma source is directly proportional to the plasma density, which is itself a function of the RF power absorbed by the plasma [9, 13]. However, increasing the RF power results in a larger ion energy spread, which negatively affects the microprobe formation due to the action of chromatic aberrations. Since a proton beam current of ~10 nA is sufficient for a compact nuclear microprobe, it becomes feasible to design a RF ion source of low power. This facilitates the operating temperature conditions of the source and reduces high-frequency electromagnetic (EM) interference that could affect electronic measuring equipment.

High EM fields can cause RF interference with the extracting and accelerating voltage power supplies, as well as generate parasitic capacitive coupling between the induction coil and the plasma. These effects may result in RF modulation of the extracted ion current and increases the ion energy spread [14].

In view of these considerations, the RF generator was designed to operate at a power level below 10 W. The generator is built using a GU–29 vacuum tube according to the scheme of a push-pull oscillator. The anode voltage of the tube is 250…280 V and current consumption of 25…30 mA, corresponding to a total power consumption of approximately 8 W. Taking into account the generator efficiency, the RF power absorbed by the plasma does not exceed 5 W.

To characterize the EM environment near the ion source, measurements of the emitted RF electric field were carried out using an Aktakom ATT–2593 field meter. The measured electric field strength was approximately 1.2 V/m at a distance of 0.5 m from the source, decreasing to around 0.75 V/m at distances of 1…1.5 m.

2. EXPERIMENTAL SETUP

All measurements of the RF ion source characteristics were carried out on the experimental setup shown in Fig. 2. The ion source was mounted on a vacuum chamber with an internal volume of approximately 6 liters. The vacuum chamber was evacuated by a turbomolecular pump Leybold–360 with a pumping speed of 360 L/s. The base pressure achieved was 1×10^{-4} Pa, as monitored by a VMB–14 vacuum gauge.

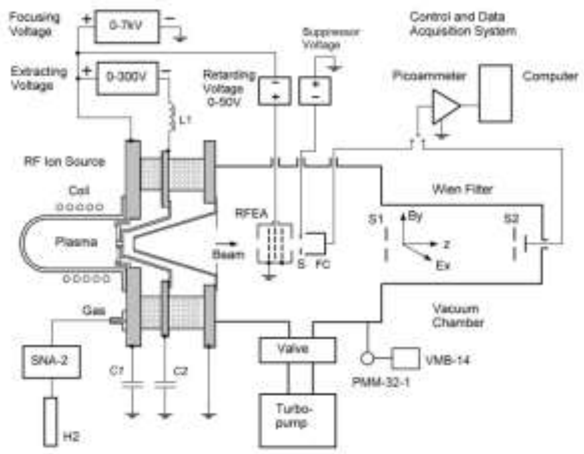

Fig. 2. Schematic diagram of the experimental setup

Hydrogen was introduced into the discharge tube of the source using the SNA–2 gas supply system. A separate experimental run was performed with a PMT–2 thermocouple sensor attached directly to the discharge bulb of the ion source. This allowed for the establishment of a correlation between the readings of the gas supply system, the pressure in the vacuum chamber, and the actual hydrogen pressure within the source bulb.

Under operational conditions, the hydrogen pressure inside the discharge tube ranged from 0.5 to 5 Pa, while the vacuum chamber pressure remained within $(3\ldots9)\cdot10^{-4}$ Pa, depending on the gas supply.

3. RESULTS AND DISCUSSION

3.1. ION BEAM CURRENT

The current-voltage (I–V) characteristics of the ion source, which represent the dependence of the ion beam current I_i on the extraction voltage U_{ext}, were measured using a Faraday cup positioned 100 mm from the ion source. The Faraday cup has an entrance aperture diameter of 22 mm and is equipped with a suppressor electrode biased to -290 V to suppress secondary electron emission.

Fig. 3 presents the measured dependence of the ion beam current I_i on the extraction voltage U_{ext} at various hydrogen pressure within the discharge tube (ranging from 1.2 to 3 Pa). The extraction voltage U_{ext} was varied from 10 to 290 V, while the accelerating voltage was maintained constant at U_{acc} =4 kV.

The obtained I–V curves exhibit a typical trend observed in RF plasma ion sources: the extracted current increases monotonically with the extraction voltage, reaches a maximum (saturation), and subsequently decreases.

The highest beam current was observed at the low pressure of p=1.2 Pa, where the current reached I_i = 3.5 μA at U_{ext}=240 V.

The ion beam current density j_i can be estimated from the relationship: $j_i = I_i / S_a$, where S_a is the area of the extraction aperture. For I_i=3.5 μA, this yields a current density of approximately j_i=1.2 mA/cm^2.

This behavior of the I–V curve is consistent with the known emission characteristics of RF plasma sources, where the emission plasma boundary takes the shape of a meniscus.

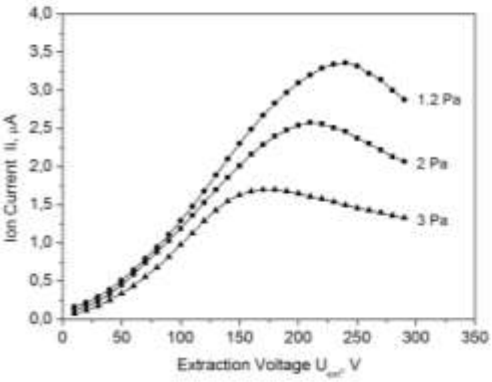

Fig. 3. Ion beam current I_i as a function of extraction voltage U_{ext} for various hydrogen pressures in the source

The geometry of the plasma meniscus changes depending on the plasma density n_e, electron temperature T_e, and the extraction voltage U_{ext}. At lower extraction voltages, the beam current follows the Child–Langmuir law, which predicts:

$$j_i = (4\varepsilon_0/9)\sqrt{2e/m}\cdot(U_{ext}^{3/2}/d^2),$$

where ε_0 is the vacuum permittivity, e is the elementary charge, m is the electron mass, d is the distance between the plasma boundary and the extraction electrode.

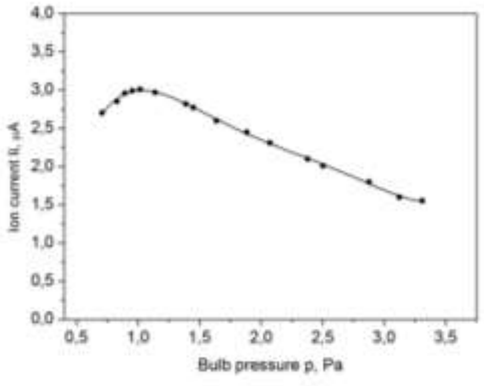

Fig. 4. Ion beam current I_i versus hydrogen pressure p in the ion source

At higher voltages, space charge limitations and changes in the plasma boundary condition cause current saturation. The saturation current density is determined as [9]:

$$j_{sat} = 0.4en_e\sqrt{kT_e/M_i},$$

where k is the Boltzmann constant, and M_i is the ion mass.

Fig. 4 shows the dependence of the ion beam current I_i on hydrogen pressure in the ion source for a fixed U_{ext}= 190 V and U_{acc}=4 kV.

As seen from the graph, the beam current exhibits a maximum at a pressure of 1.2 Pa, and then gradually decreases with increasing gas pressure.

An important operational characteristic of an ion source is the long-term stability of the extracted ion beam current. The value of random current fluctuations is defined as $\delta I_i = 2\sigma/I_{av}$, where σ is the standard deviation of the beam current, and I_{av} is the average current over the observation period.

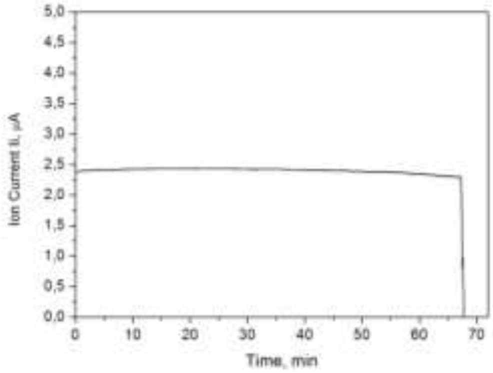

Fig. 5. Ion beam current recorded continuously over a one-hour period

Fig. 5 presents a continuous measurement of the ion beam current I_i recorded over a period exceeding one hour. The data demonstrate good temporal stability of the beam. The measured fluctuations remained below 1% during the entire observation period, indicating that the source provides a stable beam suitable for applications in microbeam systems.

3.2. MASS COMPOSITION OF THE BEAM

The mass composition of the beam was measured using a Wien filter, which is schematically shown in Fig. 2. In the Wien filter, a constant magnetic field B_y is created by the coils of the electromagnet and directed vertically. The distance between the metal poles of the electromagnet is 8 mm. A constant potential difference U_W is applied to two parallel electrostatic plates, creating an electric field E_x in the horizontal direction between them. The dimensions of the slits S1 and S2 are 1 and 0.4 mm, respectively, with a distance of 400 mm between them. As the ion beam passes through the crossed electric and magnetic fields, ion separation by mass occurs. The mass spectrum was scanned by varying the magnetic field of the Wien filter. During this process, the current of the electromagnet was linearly increased within the range of 0…2 A. The voltage applied to the electrostatic plates was U_W= ±70 V, with the midpoint grounded.

The typical mass spectrum of the ion beam is shown in Fig. 6. The spectrum was measured at U_{ext}=240 V, U_{acc}=5 kV and pressure p=1.2 Pa.

The horizontal axis represents the current of the Wien filter magnet. The masses of the analyzed ions are proportional to the square of the current. The spectrum displays characteristic peaks for hydrogen ions: $^1H^+$, $^2H^+$, and $^3H^+$. The height of the $^1H^+$ (proton) peak is

40 pA, the molecular ion peak $^2H^+$ is 200 pA, and the $^3H^+$ ion peak is 130 pA. Thus, the proton ratio in the beam is approximately 10%.

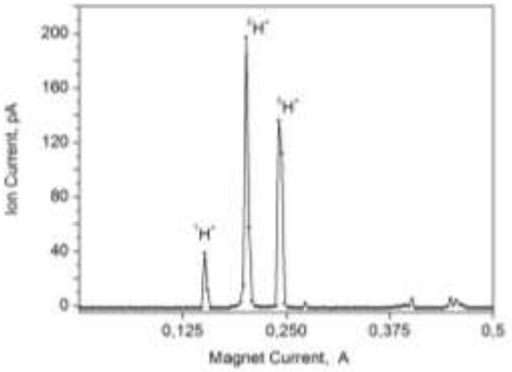

Fig. 6. Mass spectrum of the ion beam

According to the recommendations provided in [9], the conditions for achieving a high proton fraction include high RF power of the ion source and low gas pressure. Therefore, the low RF power used in this study (< 10 W) accounts for the relatively low proton ratio. Despite this, the ion source produces about 350 nA of proton current at a total beam current of 3.5 μA.

Reducing the emission orifice to below 100 μm will decrease the beam current to an acceptable level, thereby improving the spatial resolution of the microprobe.

3.3. AXIAL ION ENERGY SPREAD

The axial ion energy spread of the beam was measured using a retarding field energy analyzer (RFEA) [14, 15]. The analyzer, schematically shown in Fig. 2, consists of three flat parallel grids with 80% transparency, spaced 2 mm apart. The first and third grids are held at ground potential, while a positive retarding potential U_r is applied to the middle grid relative to the accelerating voltage.

The ion beam is collected by a Faraday cup (marked FC in Fig. 2) with a diameter of 25 mm, positioned 30 mm downstream of the third grid. The Faraday cup is equipped with an electron suppressor to eliminate the influence of secondary electrons on the current measurement. The analyzer is housed in a stainless steel cylinder with a diameter of 45 mm and a length of 50 mm. The entrance and exit apertures each have a diameter of 20 mm.

Beam energy analysis was performed by varying the retarding potential U_r from 0 to 50 V in 1 V increments, while recording the corresponding ion current *I*. The current was measured using a "Keithley 6485" picoammeter and recorded via computer interface.

The ion current *I* depends on the retarding potential U_r applied to the middle grid. The ion energy distribution function (IEDF), *f(E)*, is proportional to the negative first derivative of the ion current *I* [14]: $f(E) \propto -dI/dU_r$. The ion energy spread ΔE is defined as the full width of the distribution function at half maximum.

One of the factors contributing to the broadening of the energy distribution function is RF interference affecting both the extracting and accelerating electrodes, as well as their respective power supplies. RF fields can penetrate the plasma and the extraction regions, inducing oscillations in the plasma potential. These oscillations lead to RF modulation of the ion beam, thereby increasing the ion energy spread [9, 14]. To suppress RF-induced effects, blocking capacitors and chokes were implemented in the circuit [9, 15]. These components, marked as C1, C2, and L1 in Fig. 2, have values of C1=C2=2000 pF and L1=100 μH.

Energy spread measurements were conducted at various extraction voltages U_{ext} and hydrogen pressure *p* within the ion source. During the experiments, the extraction electrode was grounded, and no accelerating voltage was applied.

Fig. 7 presents the result of measurements at U_{ext}=200 V and *p*=1 Pa. The measured ion current *I* is plotted as discrete points, while the corresponding derivative $-dI/dU_r$, which is proportional to the IEDF, is shown as a curve with square markers.

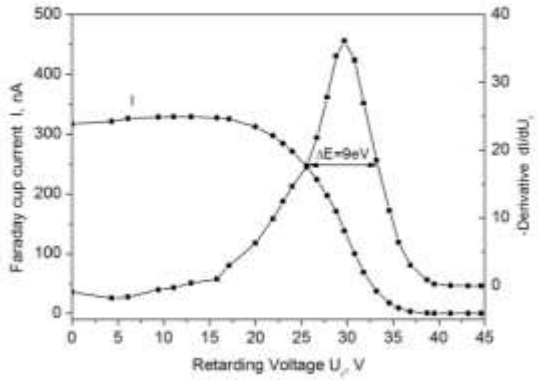

Fig. 7. Ion current I (points) and its derivative -dI/dU$_r$ (squares) versus retarding voltage U$_r$

Measurements revealed that at low pressure of *p*=1.2 Pa, the energy spread is approximately ΔE=9 eV. As the pressure increased to *p*=3.5 Pa, the energy spread decreased to about ΔE=7.5 eV. The energy spread was found to be independent of the extraction voltage within the tested range.

3.4. BEAM EMITTANCE

The emittance of an ion source is a key parameter determining the ability of the beam to focus and transport. The emittance of the RF source was measured using an electrostatic emittance scanner, the design and operation of which are described in [16]. This device is based on the Allison-type design [17–19].

The scanner consists of two parallel deflecting plates with a 10 mm gap, across which a sawtooth voltage is applied to electrostatically deflect incoming ions. The system also includes an entrance slit, an exit slit, and a Faraday cup for measuring the ion current passed through both slits. The scanner is traversed across the vertical direction (x-axis) of the beam using a stepper motor.

The deflection plates are 120 mm long in the beam propagation direction. The widths of the entrance and exit slits are 200 μm. The scanner provides a spatial resolution of 4.8 μm, a scanning range of 0…20 mm, and an angular resolution of 1.7 mrad. During the measurement, the scanner was placed 40 mm downstream of the RF source and scanned along the x-axis from 0 to 14 mm in steps of 100 μm. The deflection voltage applied to the plates was varied from -200 V to +200 V in 2 V increments, corresponding to an angular scanning range of -71 to +71 mrad.

Emittance measurements were performed under conditions corresponding to the maximum extracted ion current: extraction voltage U_{ext} = 250 V, acceleration voltage U_{acc} = 7 kV, and hydrogen pressure p=1.2 Pa.

Fig. 8 shows a 3D surface plot of the measured ion beam current intensity distribution.

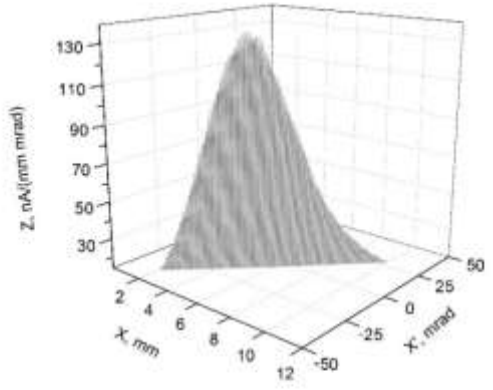

Fig. 8. 3D surface of a current intensity distribution

The corresponding emittance diagram is presented in Fig. 9, with the emittance contour enclosing 90% of the total beam current.

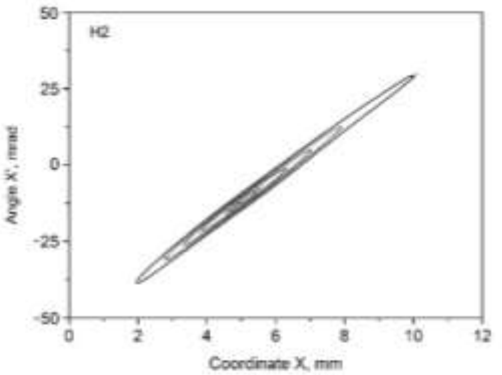

Fig. 9. Contour of ε_{90} beam emittance

At a beam energy of E=7 keV, the geometric emittance is ε_{90}= 9.8 π·mm·mrad, while the root-mean-square (rms) emittance is ε_{rms}= 2.2 mm·mrad. The ratio $\varepsilon_{90}/\varepsilon_{rms}$= 4.4 is consistent with the theoretical value of 4.6 expected for ion beams with a Gaussian intensity distribution [9, 20, 21].

The normalized emittance is given by $\varepsilon_N=\varepsilon\cdot\beta\cdot\gamma$, where β and γ are the relativistic factors. The normalized emittance is ε_N = 0.037 π·mm·mrad and it remains constant with respect to changes in beam energy.

The diverging ion beam had a diameter of 3.6 mm at a distance of 40 mm from the source. The divergence angle is 30.8 mrad.

To enable comparison between ion sources operating at different energies, the energy-normalized emittance is often used. This parameter is defined as the product $\varepsilon\cdot E^{1/2}$. For the presented RF ion source, the energy-normalized emittance is 0.8 π·mm·mrad·(MeV)$^{1/2}$. For comparison, the commercial RF ion source model SO 173 from "High Voltage Engineering Europa" exhibits energy-normalized emittance of 1.2 π·mm·mrad·(MeV)$^{1/2}$ [11].

CONCLUSIONS

The development of a compact nuclear microprobe at the IAP NAS of Ukraine requires an ion source capable of generating a stable proton ($^1H^+$) beam with a current up to 10 nA and an energy spread on the order of 10 eV. To meet these requirements, a low power inductively coupled RF ion source has been designed and tested. The key performance parameters of the source are as follows: RF power <10 W, operating frequency of 45 MHz, extracted ion current up to 3.5 μA, long-term beam current stability better than 1%, and proton fraction in the extracted beam of approximately 10%.

The source features a simple and reliable design, free of incandescent cathodes that could sputter and contaminate the internal surface of the source. Moreover, apart from the extractor, no metallic surfaces are present inside the source bulb that could reduce the proton fraction in the beam.

The low RF power improves the operating temperature conditions of the source and minimizes high-frequency electromagnetic interference with diagnostic and measurement equipment. Owing to the low RF power and the implementation of RF noise suppression techniques at the extraction and acceleration stages, the ion energy spread has been reduced to 7.5…9 eV. This level of energy spread is acceptable for compact nuclear microprobe.

The measured emittance is ε_{90}= 9.8 π·mm·mrad, with a corresponding normalized emittance of ε_N= 0.037 π·mm·mrad. The energy-normalized emittance is 0.8 π·mm·mrad·(MeV)$^{1/2}$, indicating good focusing and transport properties of the beam.

In summary, the presented RF ion source meets the key requirements for use in the injector stage of a compact nuclear microprobe at the Institute of Applied Physics of the National Academy of Sciences of Ukraine. Future work will focus on investigating the source performance with extraction apertures smaller than 100 μm to further enhance spatial resolution and microbeam quality.

The work was carried out within the framework of the project "Study of physical processes of ion beam formation in a compact nuclear microprobe based on an immersion probe forming system" under the Priority thematic area of scientific research and scientific and technical developments in Ukraine "Fundamental problems of physics, astrophysics, materials science, nuclear energy and radiation safety".

REFERENCES

1. S. Matsuyama, M. Miwa, S. Toyama, T. Kamiya, Y. Ishii, T. Satoh. Current status of the Tohoku microbeam system at Tohoku University and other facilities // *Nucl. Instr. and Meth. B.* 2023, 539, p. 79-88.

2. M. Jaksic, G. Provatas, I. Bozicevic Mihalic, A. Crnjac, D. Cosic, T. Dunatov, O. Romanenko, Z. Siketic. The dual ion beam microprobe // *Nucl. Instr. and Meth. B.* 2023, 539, p. 120-126.
3. G. Nagy, H.J. Whitlow, D. Primetzhofer. The scanning light ion microprobe in Uppsala-Status in 2022 // *Nucl. Instr. and Meth. B.* 2022, v. 533, p. 66-69.
4. A.G. Ponomarev, A.A. Ponomarov. Beam optics in nuclear microprobe: A review // *Nucl. Instr. And Meth. B.* 2021, № 497, p. 15-23.
5. I.G. Ignat’ev, D.V. Magilin, V.I. Miroshnichenko, A.G. Ponomarev, V.E. Storizhko, B. Sulkio-Cleff. Immersion probe-forming system as a way to the compact design of nuclear microprobe // *Nucl. Instr. and Meth. B.* 2005, v. 231, p. 94-100.
6. S. Kalbitzer. Bright ion beams for the nuclear microprobe // *Nucl. Instr. and Meth. B.* 1999, v. 158, p. 53-60.
7. J.A. van Kan, R. Pang, T. Basu, Y. Dou, Gokul, N. Tarino, J. Tregidga, S.C. Roy, and H.N. Tan. Considerations for the nano aperture ion source: Geometrical design and electrical control // *Rev. Sci. Instrum*. 2020, v. 91, p. 013310.
8. Y. Dou, T. Osipovicz, J.A. van Kan. Breaking the 10 nm barrier using molecular ions in nuclear microprobes // *Ultramicroscopy*. 2023, v. 253, p. 113812.
9. H. Zhang. *Ion Sources*. Science Press, Springer, New York, 1999, p. 63-72, 153-163, 313-322.
10. A. Annaluru, D.J.W. Mous, and R.C. Walet. HVE ion sources for medium and high-energy accelerator systems // *J. Phys.:* Conf. Ser. 2024, v. 2743, p. 012027.
11. RF Ion Source, Model SO 173. https://www.highvolteng.com/media/Leaflets/RFS-3.pdf
12. V.I. Voznyi, O.G. Ponomarev, V.A. Rebrov. Materials of the X All-Ukrainian Scientific and Practical Conference with International Participation, (Sumy, April 15-16, 2024), p. 13.
13. M.A. Lieberman and A.J. Lichtenberg. *Principles of Plasma Discharges and Materials Processing*. New York: Wiley: 1994, p. 308.
14. U. Kortshagen and M. Zethoff. Ion energy distribution functions in a planar inductively coupled RF discharge // *Plasma Sources Sci. Technol.* 1995, v. 4, p. 541.
15. V.I. Voznyi, V.I. Miroshnichenko, S.N. Mordyk, V.E. Storizhko, D.P. Shulha. Axial energy spread measurements of a 27.12 MHz multicusp ion source // *PAST. Series “Plasma Physics” (15).* 2009, p. 142-144.
16. V.I. Voznyi, M.O. Sayko, A.G. Ponomarev, S.O. Sadovyi, O.V. Alexenko, R.O. Shulipa. System for measuring emittance characteristics of ion sources // *East Eur. J. Phys.* 2020, v. 3, p. 46-53.
17. P.W. Allison, J.D. Sherman, and D.B. Holtkamp. An emittance scanner for intense low-energy ion beams // *IEEE Trans. Nucl. Sci.* 1983, v. 30(4), p. 2204-2206.
18. C. Poggi, E. Sartori, M. Tollin, M. Brombin, M. Zaupa, E. Fagotti, G. Serianni. Design and development of an Allison type emittance scanner for the SPIDER ion source // *Rev. Sci. Instrum*. 2020, v. 91, p. 013328.
19. C. Poggi, G. Berton, M. Brombin, F. D. Agostini, D. Fasolo, L. Franchin. First tests and commissioning of the emittance scanner for SPIDER // *Fusion Engineering and Design*. 2021, v. 168, p. 112659.
20. D.P. Moehs, J. Peters, and J. Sherman. Negative Hydrogen Ion Sources for Accelerators // *IEEE Trans. Plasma Sci.* 2005, v. 33(6), p. 1786-1798.
21. M. Reiser. *Theory and Design of Charged Particle Beams*, 2nd ed. (Weinheim: Wiley-VCH 2008), p. 53, 323.

Article received 14.04.2025

ХАРАКТЕРИСТИКИ ІОННОГО ВЧ-ДЖЕРЕЛА МАЛОЇ ПОТУЖНОСТІ

В.І. Возний, О.Г. Пономарьов, Д.В. Магілін, Д.П. Шульга, В.А. Ребров

Представлено основні характеристики індукційного іонного ВЧ-джерела малої потужності, розробленого для використання у компактному ядерному мікрозонді ІПФ НАН України. Джерело працює на частоті 45 МГц при потужності менш ніж 10 Вт. Іонний струм екстрагованого пучка дорівнює 3,5 мкА при діаметрі апертури екстракції 0,6 мм. Масовий склад пучка вимірювався за допомогою фільтра Віна. Пучок складається з $^1H^+$-, $^2H^+$- та $^3H^+$-іонів, при цьому частка протонів ($^1H^+$) становить близько 10%. У залежності від тиску водня виміряний енергетичний розкид іонів знаходиться в межах 7,5…9 еВ. Вимірювання еміттансу пучка проводилося за допомогою електростатичного сканера. Еміттанс пучка дорівнює 9,8 π·мм·мрад, нормалізований еміттанс – 0,037 π·мм·мрад.